35th Annual International Conference of the IEEE EMBS
Osaka, Japan, 3 - 7 July, 2013

Direction and Speed Tuning of Motor-Cortex Multi-Unit Activity and Local Field Potentials During Reaching Movements

Sagi Perel[1], Patrick T. Sadtler[2], Jason M. Godlove[3],
Stephen I. Ryu[4], Wei Wang[5], Aaron P. Batista[6] and Steven M. Chase[7]

Abstract— **Primary motor-cortex multi-unit activity (MUA) and local-field potentials (LFPs) have both been suggested as potential control signals for brain-computer interfaces (BCIs) aimed at movement restoration. Some studies report that LFP-based decoding is comparable to spiking-based decoding, while others offer contradicting evidence. Differences in experimental paradigms, tuning models and decoding techniques make it hard to directly compare these results. Here, we use regression and mutual information analyses to study how MUA and LFP encode various kinematic parameters during reaching movements. We find that in addition to previously reported directional tuning, MUA also contains prominent speed tuning. LFP activity in low-frequency bands (15-40Hz, LFP_L) is primarily speed tuned, and contains more speed information than both high-frequency LFP (100-300Hz, LFP_H) and MUA. LFP_H contains more directional information compared to LFP_L, but less information when compared with MUA. Our results suggest that a velocity and speed encoding model is most appropriate for both MUA and LFP_H, whereas a speed only encoding model is adequate for LFP_L.**

I. INTRODUCTION

Primary motor-cortex (M1) is the major area for harnessing neural signals for brain-computer interface (BCI) control. In recent years, single-unit activity (SUA), multi-unit activity (MUA) and local-field potentials (LFPs) have been proposed as possible control signals for BCIs. While the relationship of SUA to various movement parameters during reaching movements has been extensively studied (e.g. [1]–[7]), that of MUA and LFP is not as well understood. Several groups have studied low-frequency LFP in the time or frequency domain, concluding that it encodes hand position, direction or velocity information [8]–[13]. Studies of high-frequency LFP in the frequency-domain have shown similar results [9], [13]–[18]. Comparisons of movement related information encoded by LFP to that encoded by either SUA or MUA have resulted in contradicting results: some studies have reported that the amount of information encoded by LFP exceeds that encoded by spiking activity, while other studies report less movement related information in LFP than in spiking.

Several factors could account for this discrepancy. First, experimental paradigms differ across the various groups. Second, while some studies used averaged neural activity, others used instantaneous activity. Third, some studies decoded kinematics from neural activity, while others used mutual-information (MI) or linear correlation based analyses. Finally, each of the studies made different assumptions about the encoding model.

Here, we extend previous work by systematically studying tuning properties of LFP and comparing them to MUA tuning. Motor-cortical SUA has been previously shown to encode both direction and speed [5]. We therefore considered tuning models which included direction, velocity, speed and their additive combinations. We used instantaneous neural activity and kinematics, as opposed to averaged data, to make our conclusions more relevant for real-time BCI use. We found that MUA exhibited prominent speed tuning, along with directional tuning which was especially evident in a small subset of the channels examined. Low- and high-frequency LFP were speed tuned. Some high-frequency LFP channels demonstrated directional tuning similar to that of MUA.

II. METHODS

A. Behavioral Task and Data Collection

A Rhesus monkey was trained to perform center-out movements using the arm contralateral to the recording site. The animal was comfortably seated in a primate chair, in front of a computer screen, with one arm restrained and the other free to move behind the screen, thus obscured from the animal. An active marker system (Phasespace Inc, San Leandro, CA) was used to track its hand position in real-time. This 3D position was projected to a 2D plane and was used to render a cursor on the computer screen in real-time. At the beginning of each trial, a center target appeared and the animal had to move its hand so that the cursor

*The work of S. Perel and S. M. Chase was supported by the Defense Advanced Research Projects Agency (DARPA) and SPAWAR System Center Pacific (SSC Pacific) under Contract No. N66001-12-C-4027. Any opinions, findings and conclusions or recommendations expressed in this material are those of the author(s) and do not necessarily reflect the views of the Defense Advanced Research Projects Agency (DARPA) and SPAWAR System Center Pacific (SSC Pacific). The work of P. T. Sadtler, J. M. Godlove and A. P. Batista was supported by the Burroughs Welcome Fund and CRCNS NSF NS-11-006. The work of P. T. Sadtler was also supported by IGERT NSF DGE-0549352. The work of W. Wang was supported by National Institutes of Health (NIH) Grants 3R01NS050256-05S1 and 8KL2TR000146-07.

[1]Sagi Perel is with the Department of Biomedical Engineering and Center for the Neural Basis of Cognition, Carnegie Mellon University, Pittsburgh, PA, 15213, USA (email: sagi@cmu.edu)

[2]Patrick T. Sadtler, [3]Jason Godlove and [6]Aaron Batista are with the Department of BioEngineering, University of Pittsburgh, Pittsburgh, PA, 15213, USA

[4]Stephen I. Ryu is with the Department of Electrical Engineering, Stanford University, Stanford, CA and the Department of Neurosurgery, Palo Alto Medical Foundation, Palo Alto, CA, USA

[5]Wei Wang is with the Department of Physical Medicine and Rehabilitation, School of Medicine, University of Pittsburgh, Pittsburgh, PA, 15213, USA

[7]Steven M. Chase is with the Department of Biomedical Engineering and Center for the Neural Basis of Cognition, Carnegie Mellon University, Pittsburgh, PA, 15213, USA (email: schase@cmu.edu)

978-1-4577-0216-7/13/$26.00 ©2013 IEEE

location matched the center target. Then, after 200-400ms, a peripheral target appeared. The animal reached so the cursor moved to the peripheral target, within ~800ms, or else the trial would fail. Successful trials were indicated with a water reward. On some trials, the animal had to move its hand so the cursor followed paths of varying shapes and thicknesses. On most trials, the hand path was not constrained. Neural tuning did not seem to differ between these two tasks, so those data were combined for the analyses described here.

After the animal had sufficient proficiency in the task, a 96-electrode silicon array (Blackrock Systems Inc.) was chronically implanted in the arm region of the contralateral motor-cortex. All surgical procedures followed protocols approved by the University of Pittsburgh Institutional Animal Care and Use Committee. Post-surgery, the animal resumed performing the task while neural activity was recorded and stored for off-line analysis using a TDT system (Tucker-Davis Technologies, Florida). The 3D hand position (sampled at 120Hz) and relevant task information were stored in synchronization with the neural data.

An RMS based threshold was used to obtain threshold-crossing event times for every channel. Here, we refer to these threshold-crossing events as MUA, but that does not necessarily imply these are multi-unit clusters of neural activity that are well separated from the noise floor. LFP activity was obtained by band-pass filtering channel voltage signals (10-500Hz), and was stored at a sampling rate of 1220Hz. Off-line, MUA threshold-crossings were converted to firing-rates by counting events in consecutive 100ms bins and dividing by the bin width. The LFP power-spectral density (PSD) was computed at a temporal resolution of 16ms with a frequency resolution of 5Hz using the mem library (BCI2000 Project [19]), and then log-transformed. In the analyses presented in this paper, we used two frequency-bands: 15-40Hz (LFP_L) and 100-300Hz (LFP_H). These two bands demonstrate the two major types of modulation commonly found in LFP during reaching movements (suppression and facilitation relative to baseline, e.g. [20]). Due to noise artifacts in the frequency band 28-32Hz, these frequencies were notch-filtered prior to computing the LFP PSD. We chose the LFP_L and LFP_H frequency bands based on both single channel and channel averaged normalized time frequency plots. We found that frequencies in these ranges tended to demonstrate similar tuning (data not shown). Furthermore, R^2 values for the 41-99Hz band (see sec. II-B) were significantly lower compared to the other two bands, hence we ignored it in further analyses.

B. Tuning Models Estimation

Based on previous studies, suggesting that SUA contains both directional and speed information [5], we considered the following 5 tuning models:

$$y = b_0 + b_x d_x + b_y d_y + noise \quad (1)$$

$$y = b_0 + b_x v_x + b_y v_y + noise \quad (2)$$

$$y = b_0 + b_s s + noise \quad (3)$$

$$y = b_0 + b_x d_x + b_y d_y + b_s s + noise \quad (4)$$

$$y = b_0 + b_x v_x + b_y v_y + b_s s + noise \quad (5)$$

where:

- y is a single-channel MUA instantaneous firing-rate in Hz, or a single channel log-transformed instantaneous LFP PSD averaged across a given frequency band
- $\vec{d} = (d_x, d_y) = (cos(\theta), sin(\theta))$ is the instantaneous direction of hand movement
- $\vec{v}$ is the instantaneous hand velocity
- $s = |\vec{v}|$ is the instantaneous hand speed

These models relate neural activity to instantaneous direction (eq. 1), velocity (eq. 2), speed (eq. 3), direction & speed (eq. 4), and velocity & speed (eq. 5). Together, they allow systematic investigation of how MUA and LFP relate to direction and speed components in a multiplicative or additive manner. Prior to fitting the regression models, MUA firing-rate and kinematic features were spline-interpolated to match the LFP PSD sampling frequency. We also performed a lag analysis, where we fit the above models with varying lags between the neural and kinematic features. We considered lags ranging from causal values (-300ms) to non-causal values (+400ms), at 50ms steps. For most MUA channels, the best fits, as determined by coefficient of determination (R^2) values, were obtained with causal lags in the range of -100 to -150ms. For real-time BCI control, a single time-lag would likely be used for all channels; therefore we chose a causal lag of 100ms for all channels (MUA and LFP), for all analyses in this paper.

C. Mutual Information Estimation

The models in eq. 1-5 explore the linear relationship between neural activity (MUA, LFP) and velocity, direction and/or speed. However, if neural activity is linearly related to velocity, then it might be non-linearly related to its magnitude (speed). We therefore explored non-linear relationships between neural and kinematic features, in the form of mutual-information (MI), which measures any dependency between two random variables, regardless of its functional form. MI was empirically estimated by:

$$MI(X;Y) = \sum_{x \in X} \sum_{y \in Y} p(x,y) log(\frac{p(x,y)}{p(x)p(y)}) \quad (6)$$

where:

- Y represents single-channel instantaneous neural activity
- X represents instantaneous direction or speed

Empirical MI estimations are sensitive to data discretization, hence we chose the following discretization schemes. Given that the behavioral task used peripheral targets at roughly 8 regions around the center target, we discretized movement direction (θ) to 8 bins. To ensure similar entropy for direction and speed, speed was discretized to 8 bins as well. We used varying bin widths resulting in close to uniform marginal distributions for direction and speed. For Y, we used MUA spike counts in $100ms$ bins, or discretized LFP PSD for a given frequency-band.

Empirical MI estimates tend to be positively biased [21]. We estimated this bias by permuting the neural data and computing the MI to direction and speed 100 times; then computing the bias as the mean of these 100 null MI values. This bias estimate was then subtracted from the MI estimate, for every channel and neural data type, in all the analyses described here.

To determine an optimal discretization for LFP PSD, we computed the bias-corrected MI using 5-305 bins (in steps of 5). As expected, both the MI and bias increased with the number of bins, but bias-corrected MI estimates for all LFP channels and frequency bands tended to plateau for more than 25 bins. We therefore discretized LFP PSD using 25 bins.

III. RESULTS

A. Linear Tuning to Kinematics

We first explored linear tuning of MUA and LFP to direction, velocity and speed using the regression models from sec. II-B. We fit the models using data from multiple recording sessions and results were qualitatively similar. We chose to present data from the two sessions with the largest number of trials. Fig. 1 summarizes our findings in the form of R^2 box-plots across all channels, one for every model and neural modality (MUA, LFP_L, LFP_H). It should be noted that R^2 values are lower than those previously reported using averaged data, because we used instantaneous non-smoothed data, as would be the case in on-line BCI control.

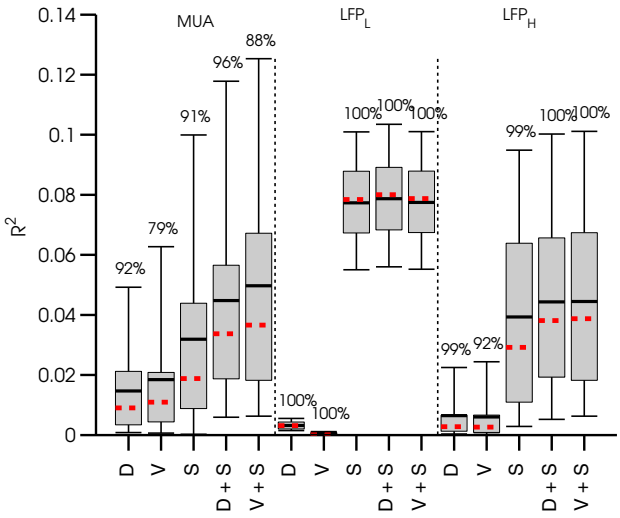

Fig. 1. **MUA and LFP Tuning Model R^2.** Population tuning model R^2 for the 5 models described in sec. II-B: Direction (D), Velocity (V), Speed (S), Direction & Speed (D+S), Velocity & Speed (V+S). Box-plots describe the 5^{th}, 25^{th}, 75^{th} and 95^{th} R^2 percentiles, as well as the mean (solid line) and median (dashed line) R^2, across all channels with significant regressions. Percentages above the 95^{th} percentile indicate the proportion of significant regressions among 87 channels. MUA demonstrates the strongest direction and velocity tuning. MUA speed tuning is prominent. Most LFP_L and LFP_H channels are speed tuned. Some LFP_H channels show direction and velocity tuning, equivalent to MUA. LFP_L shows the strongest speed tuning across the three modalities.

While previously published results indicated that SUA encodes direction or velocity [5], [11], [17], we found that MUA encoded speed better than either direction or velocity, possibly due to the fact that threshold-crossing events in MUA originated from multiple single-units with different directional tuning. The two models incorporating direction & speed (eq. 4) or velocity & speed (eq. 5) yielded the highest R^2 values across MUA channels. These models were better than either speed, direction, or velocity only models, indicating that MUA encoded directional information which was independent of speed information. The differences between the mean and median R^2 for all models indicated that the R^2 distribution has a long positive tail. Therefore, MUA tuning was heterogeneous, where a small subset of channels (~20%) encoded the kinematic features better than the other channels.

We found that LFP_L encoded only speed, with no evidence of directional tuning. The difference between the LFP_L mean and median R^2 was very small, suggesting that LFP_L speed tuning was homogeneous, in the sense that most channels encoded speed equally well. Most LFP_H channels contained prominent speed tuning, but in contrast to LFP_L, a subset of channels (~20%) were also directionally tuned.

Fig. 1 also allows us to compare tuning across neural modalities. As expected, most MUA channels encoded direction and velocity better than either LFP_L or LFP_H channels. A subset of LFP_H channels (~20%) demonstrated direction or velocity R^2 values equivalent to the average MUA R^2. Speed was best encoded by LFP_L: the worst LFP_L channels encoded speed better than ~80% of MUA channels and ~70% of LFP_H channels.

B. Non-Linear Tuning to Kinematics

We used the information theoretic analysis described in sec. II-C to capture potential non-linear dependencies between MUA, LFP_L, LFP_H and direction or speed, beyond the linear tuning described in sec. III-A. Fig. 2 shows box-plots of MI values across all channels and neural modalities. The results in Fig. 2 are qualitatively similar to Fig. 1. Direction was best encoded by MUA, followed by a subset of LFP_H channels with weaker direction encoding. While $MI(LFP_L;direction)$ was very low, $MI(LFP_L;speed)$ was higher than $MI(MUA;direction)$. $MI(MUA;speed)$ and $MI(LFP_H;speed)$ were similar across channels, both lower than $MI(LFP_L;speed)$. These results support the tuning analyses in sec. III-A, suggesting that linear models adequately describe the relationships between MUA, LFP and speed or direction.

IV. DISCUSSION

Multi-unit activity (MUA) and local-field potentials (LFPs) are two potential control signals for brain-computer interfaces. Recent studies relating MUA and LFP to various movement kinematics resulted in disagreement. Some studies suggest that LFP based decoding is equivalent to MUA based decoding, while other studies have found MUA based decoding to be superior. One possible reason for the contradicting results is the different tuning models used in those studies. Another reason could be data pre-processing:

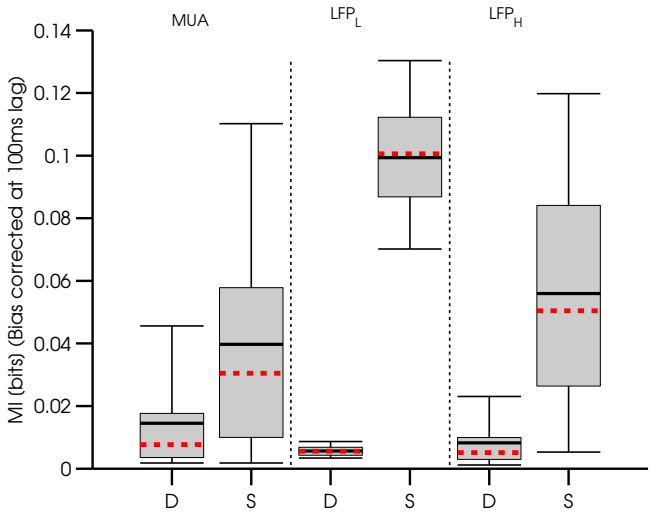

Fig. 2. **MUA and LFP MI Comparison.** MI between MUA, LFP_L, LFP_H and kinematics (direction and speed) is compared. MI between MUA and direction is the highest among the three modalities. MI between LFP_L and speed is the highest among the three modalities. Compare to fig. 1 where linear tuning is shown.

some studies used averaged data, others applied different filters to instantaneous data. The relative time-lags between neural data and kinematics also varied across studies.

Here, we studied a rich set of MUA and LFP encoding models using instantaneous non-filtered data, with a fixed lag, to closely match the type of data used in on-line BCI studies. We found that while MUA was directionally tuned, as previously reported, it was more strongly tuned to speed. Based on this finding, decoding models utilizing MUA would benefit from taking speed tuning into account. A velocity-speed encoding model (eq. 5) best represented MUA tuning in our data. MUA tuning was heterogenous across channels: some channels encoded speed or direction much better than others. This suggests that BCI decoding might also benefit from some form of channel selection criteria.

Of the models we tested, we found that our low-frequency LFP activity (LFP_L) was driven predominantly by speed, and that LFP_L activity across channels was highly correlated. High-frequency LFP activity (LFP_H) encoded both speed and direction, although directional information was lower compared to MUA. LFP_H activity across electrodes was more heterogenous compared to LFP_L: similarly to MUA, a subset of LFP_H channels best encoded speed or direction. We determined that the most appropriate LFP_L encoding model was a speed only model (eq. 3), whereas a velocity-speed encoding model (eq. 5) best described LFP_H tuning.

Our regression and mutual-information analyses showed similar trends for both MUA and LFP, suggesting that linear direction and speed models adequately capture the neural tuning in our data. Based on our findings, a hybrid MUA-LFP decoder, accounting for the prominent speed tuning in both neural modalities, should prove superior to velocity-only based decoders.

References

[1] A. P. Georgopoulos, J. F. Kalaska, R. Caminiti, and J. T. Massey, "On the relations between the direction of two-dimensional arm movements and cell discharge in primate motor cortex," *J Neurosci*, vol. 2, no. 11, pp. 1527–37, 1982.

[2] D. Flament and J. Hore, "Relations of motor cortex neural discharge to kinematics of passive and active elbow movements in the monkey," *J Neurophysiol*, vol. 60, no. 4, pp. 1268–84, 1988.

[3] Q. G. Fu, D. Flament, J. D. Coltz, and T. J. Ebner, "Temporal encoding of movement kinematics in the discharge of primate primary motor and premotor neurons," *J Neurophysiol*, vol. 73, no. 2, pp. 836–54, 1995.

[4] S. H. Scott, L. E. Sergio, and J. F. Kalaska, "Reaching movements with similar hand paths but different arm orientations. ii. activity of individual cells in dorsal premotor cortex and parietal area 5," *J Neurophysiol*, vol. 78, no. 5, pp. 2413–26, 1997.

[5] D. W. Moran and A. B. Schwartz, "Motor cortical representation of speed and direction during reaching," *J Neurophysiol*, vol. 82, no. 5, pp. 2676–92, 1999.

[6] L. Paninski, M. R. Fellows, N. G. Hatsopoulos, and J. P. Donoghue, "Spatiotemporal tuning of motor cortical neurons for hand position and velocity," *J Neurophysiol*, vol. 91, no. 1, pp. 515–32, 2004.

[7] L. Paninski, "Superlinear population encoding of dynamic hand trajectory in primary motor cortex," *Journal of Neuroscience*, vol. 24, no. 39, pp. 8551–8561, 2004.

[8] C. Mehring, J. Rickert, E. Vaadia, S. C. de Oliveira, A. Aertsen, and S. Rotter, "Inference of hand movements from local field potentials in monkey motor cortex," *Nature Neuroscience*, vol. 6, no. 12, pp. 1253–1254, 2003.

[9] J. Rickert, S. C. Oliveira, E. Vaadia, A. Aertsen, S. Rotter, and C. Mehring, "Encoding of movement direction in different frequency ranges of motor cortical local field potentials," *J Neurosci*, vol. 25, no. 39, pp. 8815–24, 2005.

[10] I. Asher, E. Stark, M. Abeles, and Y. Prut, "Comparison of direction and object selectivity of local field potentials and single units in macaque posterior parietal cortex during prehension," *J Neurophysiol*, vol. 97, no. 5, pp. 3684–95, 2007.

[11] E. Stark and M. Abeles, "Predicting movement from multiunit activity," *Journal of Neuroscience*, vol. 27, no. 31, pp. 8387–8394, 2007.

[12] A. K. Bansal, C. E. Vargas-Irwin, W. Truccolo, and J. P. Donoghue, "Relationships among low-frequency local field potentials, spiking activity, and three-dimensional reach and grasp kinematics in primary motor and ventral premotor cortices," *J Neurophysiol*, vol. 105, no. 4, pp. 1603–19, 2011.

[13] J. Liu and W. T. Newsome, "Local field potential in cortical area mt: stimulus tuning and behavioral correlations," *J Neurosci*, vol. 26, no. 30, pp. 7779–90, 2006.

[14] D. A. Heldman, W. Wang, S. S. Chan, and D. W. Moran, "Local field potential spectral tuning in motor cortex during reaching," *IEEE Trans Neural Syst Rehabil Eng*, vol. 14, no. 2, pp. 180–3, 2006.

[15] J. Zhuang, W. Truccolo, C. Vargas-Irwin, and J. P. Donoghue, "Reconstructing grasping motions from high-frequency local field potentials in primary motor cortex," *Conf Proc IEEE Eng Med Biol Soc*, vol. 2010, pp. 4347–50, 2010.

[16] ——, "Decoding 3-d reach and grasp kinematics from high-frequency local field potentials in primate primary motor cortex," *IEEE Trans Biomed Eng*, vol. 57, no. 7, pp. 1774–84, 2010.

[17] R. D. Flint, E. W. Lindberg, L. R. Jordan, L. E. Miller, and M. W. Slutzky, "Accurate decoding of reaching movements from field potentials in the absence of spikes," *J Neural Eng*, vol. 9, no. 4, p. 046006, 2012.

[18] A. K. Bansal, W. Truccolo, C. E. Vargas-Irwin, and J. P. Donoghue, "Decoding 3d reach and grasp from hybrid signals in motor and premotor cortices: spikes, multiunit activity, and local field potentials," *J Neurophysiol*, vol. 107, no. 5, pp. 1337–55, 2012.

[19] G. Schalk, D. J. McFarland, T. Hinterberger, N. Birbaumer, and J. R. Wolpaw, "Bci2000: a general-purpose brain-computer interface (bci) system," *IEEE Trans Biomed Eng*, vol. 51, no. 6, pp. 1034–43, 2004.

[20] M. Mollazadeh, V. Aggarwal, A. G. Davidson, A. J. Law, N. V. Thakor, and M. H. Schieber, "Spatiotemporal variation of multiple neurophysiological signals in the primary motor cortex during dexterous reach-to-grasp movements," *J Neurosci*, vol. 31, no. 43, pp. 15 531–43, 2011.

[21] A. Treves and S. Panzeri, "The upward bias in measures of information derived from limited data samples," *Neural Computation*, vol. 7, no. 2, pp. 399–407, 1995.